

Parameters of scalar resonances from the combined analysis of data on processes $\pi\pi \rightarrow \pi\pi, K\bar{K}, \eta\eta$ and J/ψ decays

Yurii S. Surovtsev,¹ Petr Bydžovský,² Robert Kamiński,³ Valery E. Lyubovitskij,^{4,5} and Miroslav Nagy⁶

¹*Bogoliubov Laboratory of Theoretical Physics, Joint Institute for Nuclear Research, 141 980 Dubna, Russia*

²*Nuclear Physics Institute, Czech Academy of Sciences, 25068 Řež, Czech Republic*

³*Institute of Nuclear Physics, Polish Academy of Sciences, Cracow 31342, Poland*

⁴*Institut für Theoretische Physik, Universität Tübingen, Kepler Center for Astro and Particle Physics, Auf der Morgenstelle 14, D-72076 Tübingen, Germany*

⁵*Department of Physics, Tomsk State University, 634050 Tomsk, Russia*

⁶*Institute of Physics, Slovak Academy of Sciences, Bratislava 84511, Slovak Republic*

(Received 3 December 2013; published 28 February 2014)

A combined analysis of data on the isoscalar S -wave processes $\pi\pi \rightarrow \pi\pi, K\bar{K}, \eta\eta$ and on decays $J/\psi \rightarrow \phi\pi\pi, \phi K\bar{K}$ from the DM2, Mark III, and BES II Collaborations is performed to study f_0 mesons. The method of analysis is based on analyticity and unitarity and uses an uniformization procedure. In the analysis limited only to the multichannel $\pi\pi$ -scattering data, two possible sets of parameters of the $f_0(500)$ were found: In both cases the mass was about 700 MeV but the total width was either about 680 or 1040 MeV. The extension of the analysis using only the DM2 and Mark III data on the J/ψ decays does not allow us to choose between these sets. However, the data from BES II on the di-pion mass distribution in the decay $J/\psi \rightarrow \phi\pi^+\pi^-$ clearly prefer the wider $f_0(500)$ state. Spectroscopic implications from the results of the analysis are also discussed.

DOI: [10.1103/PhysRevD.89.036010](https://doi.org/10.1103/PhysRevD.89.036010)

PACS numbers: 11.55.Bq, 11.80.Gw, 12.39.Mk, 14.40.-n

I. INTRODUCTION

A comprehension of the nature of the scalar mesons is very important for some major topics in particle physics such as the QCD vacuum. However, both parameters of the scalar mesons, obtained from experimental data in various analyses, and even the status of some of them, are still quite ambiguous [1,2]. As for the meson parameters, let us mention the widely discussed $f_0(500)/\sigma$ meson [formerly $f_0(600)$], $f_0(980)$, and $f_0(1500)$. A doubtful meson existence can be demonstrated on the case of the $f_0(1370)$ state which is apparently required by a bulk of data [3], but in some analyses of only the $\pi\pi$ scattering no evidence for its existence was found [4]. We have shown that the existence of the $f_0(1370)$ does not contradict the data on $\pi\pi \rightarrow \pi\pi, K\bar{K}, \eta\eta, \eta\eta'$ [2]. In the hidden gauge unitary approach, the $f_0(1370)$ appears dynamically generated as a $\rho\rho$ state [5] and the $f_0(1710)$ as generated from the $K^*\bar{K}^*$ interaction.

Note also a situation with scalar states in the 1500-MeV region. In our previous model-independent analyses of $\pi\pi \rightarrow \pi\pi, K\bar{K}, \eta\eta(\eta\eta')$, we observed a wide state $f_0(1500)$ whereas in some other analyses, which included mainly meson production and decay processes and which are cited in the PDG tables [1], a rather narrow $f_0(1500)$ was obtained. We have suggested that the wide $f_0(1500)$, observed in the multichannel $\pi\pi$ scattering, is effectively a superposition of two states, the wide and narrow state. The latter is observed only in decays and productions of mesons. This suggestion was verified in the model-independent

two-channel analysis of data on $\pi\pi \rightarrow \pi\pi, K\bar{K}$ [6]. In the presented article, we confirm this assumption in the three-channel analysis of data on $\pi\pi \rightarrow \pi\pi, K\bar{K}, \eta\eta$ and decays $J/\psi \rightarrow \phi\pi\pi, \phi K\bar{K}$ from the DM2, Mark III, and BES II Collaborations [7–9]. This is necessary, especially as the wide states provoke many questions which should be answered.

In view of this situation related to parameters and the status of the scalar mesons, there are still many unsolved problems as to determining a QCD nature of the mesons and their assignment to the quark-model configurations in spite of a big amount of work devoted to these problems (see, e.g., [10] and references therein).

In this article, we describe the multichannel $\pi\pi$ scattering ($\pi\pi \rightarrow \pi\pi, K\bar{K}, \eta\eta$) using the method based only on the first principles, analyticity and unitarity [11], which allows us to avoid any theoretical prejudice in extracting the resonance parameters. This we call “the model independence” [2,6,12]. The method is applied to the analysis of experimental data on the multichannel $\pi\pi$ scattering and decays $J/\psi \rightarrow \phi\pi\pi, \phi K\bar{K}$. The J/ψ decays are described using a formalism from Refs. [13,14], where certain reasonable assumptions about the final-state interactions are made. Considering the obtained arrangement of resonance poles on the Riemann-surface sheets, the constants of resonance couplings with the channels, and the resonance masses, we can draw definite conclusions about the nature of the investigated states.

The article is organized as follows. A basic formalism for the three-channel model-independent method was already

given in our previous paper [2]; therefore, in Sec. II we give only formulas introducing parameters determined in the analysis. Results of the combined coupled-channel analysis of data on isoscalar S -wave processes $\pi\pi \rightarrow \pi\pi$, $K\bar{K}$, $\eta\eta$ and on decays $J/\psi \rightarrow \phi\pi\pi$, $\phi K\bar{K}$ are presented in Sec. III. Discussion of the results and conclusions are given in Sec. IV.

II. THE THREE-COUPLED-CHANNEL FORMALISM IN MODEL-INDEPENDENT APPROACH WITH UNIFORMIZING VARIABLE

The multichannel S matrix can be described in our model-independent method, which essentially utilizes a uniformizing variable, without any approximations only in the two-channel case. In the three-channel case, a four-sheeted model of the eight-sheeted Riemann surface has to be constructed to obtain a simple symmetric (easily interpreted) picture of the resonance poles and zeros of the S matrix on the uniformization plane. The matrix elements S_{ij} , where $i, j = 1, 2, 3$ denote the channel numbers, have the right-hand cuts along the real axis of the s complex plane (s is the invariant total energy squared) starting with the channel thresholds s_i and the left-hand cuts related to crossed channels. An influence of the lowest branch point s_1 ($\pi\pi$) is neglected but unitarity on the $\pi\pi$ cut is kept. Sheets of the Riemann surface are numbered according to the signs of analytic continuations of the square roots $\sqrt{s-s_i}$ as follows: $\text{signs}(\text{Im}\sqrt{s-s_1}, \text{Im}\sqrt{s-s_2}, \text{Im}\sqrt{s-s_3}) = + + +, - + +, - - +, + - +, + - -, - - -, - + -, + + -$ correspond to sheets I, II, ..., VIII, respectively.

Resonances are described on the Riemann surface using the formulas for analytic continuations of the S -matrix elements to all sheets. The formulas allow us to express the matrix elements on the unphysical sheets by means of the matrix elements on the physical sheet that have only the resonance zeros (aside the real axis), at least, around the physical region [2,11]. Assuming the resonance zeros on sheet I, we can obtain an arrangement of poles and zeros of the resonance on the whole Riemann surface which we denote as a resonance cluster. In the three-channel case, we obtain *seven types* of the resonance clusters corresponding to possible situations when there are resonance zeros on sheet I only in S_{11} -(a); S_{22} -(b); S_{33} -(c); S_{11} and S_{22} -(d); S_{22} and S_{33} -(e); S_{11} and S_{33} -(f); S_{11} , S_{22} , and S_{33} -(g). A three-channel resonance has to be described by one of the seven types of the resonance clusters which is the necessary and sufficient condition for its existence. The resonances of types (a), (b), and (c) can be related to the resonances represented by Breit-Wigner forms, but the types (d), (e), (f), and (g) do not have their equivalents in the Breit-Wigner description.

The cluster type is related to the nature of state. Considering the $\pi\pi$, $K\bar{K}$ and $\eta\eta$ channels, e.g., a resonance coupled relatively more strongly to the $\pi\pi$ channel than to

the $K\bar{K}$ and $\eta\eta$ channels is described by the cluster of type (a) but in the opposite case, the resonance is represented by the cluster of type (e) (e.g., the state with the dominant $s\bar{s}$ component). The glueball must be represented by the cluster of type (g) as a necessary condition for the ideal case.

It is also possible to distinguish, in a model-independent way [11,13], a bound state of colorless particles (e.g., $K\bar{K}$ molecule) from a $q\bar{q}$ bound state. Alike in the one-channel case, the existence of the particle bound state means presence of a pole on the real axis below the threshold on the physical sheet. In the two-channel case, therefore, the existence of the bound state in channel 2 (e.g., $K\bar{K}$ molecule) that can decay into channel 1 ($\pi\pi$ decay) implies the presence of the pair of complex conjugate poles on sheet II below the second-channel threshold without the corresponding shifted pair of poles on sheet III. In the three-channel case, the bound state in channel 3 ($\eta\eta$) that can decay into the channels 1 ($\pi\pi$ decay) and 2 ($K\bar{K}$ decay) is represented by the pair of complex conjugate poles on sheet II and by the pair of shifted poles on sheet III below the $\eta\eta$ threshold without the corresponding poles on sheets VI and VII.

The formulas of the analytic continuations [2,11] prescribe that the resonance parameters (mass, total width, and coupling constants with the channels) must be calculated using the pole positions on sheets II, IV, and VIII because only on these sheets do the analytic continuations have the forms: $\propto 1/S_{11}^I$, $\propto 1/S_{22}^I$ and $\propto 1/S_{33}^I$, respectively, i.e., the positions of poles on these sheets are at the same points of the complex-energy plane as the resonance zeros on the physical sheet. The other pole positions are shifted due to the coupling of channels.

The S -matrix elements of all coupled processes are expressed in terms of the Jost matrix determinant $d(\sqrt{s-s_1}, \dots, \sqrt{s-s_n})$ using the Le Couteur-Newton relations [15]. The Jost determinant is a real analytic function with the only square-root branch points at $\sqrt{s-s_i} = 0$. The important branch points, which correspond to the thresholds of the coupled and crossed channels, are taken into account in the uniformizing variable. In the uniformizing variable used here we neglect the lowest $\pi\pi$ -threshold branch point but take into account the threshold branch points related to the two remaining channels, and the left-hand branch point at $s = 0$ [2],

$$w = \frac{\sqrt{(s-s_2)s_3} + \sqrt{(s-s_3)s_2}}{\sqrt{s(s_3-s_2)}}, \quad (1)$$

here $s_2 = 4m_K^2$, $s_3 = 4m_\eta^2$. This variable maps our model of the eight-sheeted Riemann surface onto the uniformization w plane divided into two parts by a unit circle centered at the origin. The semisheets I (III), II (IV), V (VII), and VI (VIII) are mapped onto the exterior (interior) of the unit disk in the first, second, third, and fourth quadrants, respectively.

The physical region extends from the $\pi\pi$ threshold $i(m_\eta\sqrt{m_K^2 - m_\pi^2} + m_K\sqrt{m_\eta^2 - m_\pi^2})/m_\pi\sqrt{m_\eta^2 - m_K^2}$ on the imaginary axis along this axis down to the point i on the unit circle ($K\bar{K}$ threshold). Then it goes along the unit circle clockwise in the first quadrant to point 1 on the real axis ($\eta\eta$ threshold) and then along the real axis to the point $b = (\sqrt{m_\eta + m_K})/\sqrt{m_\eta - m_K}$ which is an image of $s = \infty$. The intervals $(-\infty, -b]$, $[-b^{-1}, b^{-1}]$, $[b, \infty)$ are the images of the corresponding edges of the left-hand cut of the $\pi\pi$ -scattering amplitude. Each resonance is represented in S_{11} by the poles and zeros that are symmetric to each other with respect to the imaginary axis. The representations of all possible types of resonances in S_{11} on the w plane can be found in Ref. [2].

The main model-independent effect of multichannel resonances is given by the pole clusters. Assuming that possible small remaining (model-dependent) contributions of resonances can be included via the background, the S -matrix elements are taken as the products

$$S = S_B S_{\text{res}}, \quad (2)$$

where S_B describes the background and S_{res} the resonance contributions.

On the w plane, the Le Couteur-Newton relations are somewhat modified taking account of the used model of the initial eight-sheeted Riemann surface

$$\begin{aligned} S_{11} &= \frac{d^*(-w^*)}{d(w)}, & S_{22} &= \frac{d(-w^{-1})}{d(w)}, \\ S_{33} &= \frac{d(w^{-1})}{d(w)}, & S_{11}S_{22} - S_{12}^2 &= \frac{d^*(w^{*-1})}{d(w)}, \\ S_{11}S_{33} - S_{13}^2 &= \frac{d^*(-w^{*-1})}{d(w)}, & S_{22}S_{33} - S_{23}^2 &= \frac{d(-w)}{d(w)}, \end{aligned} \quad (3)$$

where the subscripts in the matrix elements S_{ij} denote the channels: $i, j = 1-\pi\pi, 2-K\bar{K}, 3-\eta\eta$. The $d(w)$ function for the resonance part in these relations is

$$d_{\text{res}}(w) = w^{-\frac{M}{2}} \prod_{r=1}^M (w + w_r^*) \quad (4)$$

with M a number of resonance zeros. For the background part S_B , the d function has the form

$$d_B = \exp \left[-i \sum_{n=1}^3 \frac{\sqrt{s - s_n}}{2m_n} (\alpha_n + i\beta_n) \right], \quad (5)$$

where

$$\begin{aligned} \alpha_n &= a_{n1} + a_{n\sigma} \frac{s - s_\sigma}{s_\sigma} \theta(s - s_\sigma) + a_{nv} \frac{s - s_v}{s_v} \theta(s - s_v), \\ \beta_n &= b_{n1} + b_{n\sigma} \frac{s - s_\sigma}{s_\sigma} \theta(s - s_\sigma) + b_{nv} \frac{s - s_v}{s_v} \theta(s - s_v), \end{aligned} \quad (6)$$

with s_σ the $\sigma\sigma$ threshold and s_v the effective threshold due to the opening of many channels in the energy region around 1.5 GeV (e.g., $\eta\eta', \rho\rho, \omega\omega$). These thresholds are determined in the analysis.

The expressions (3) and (4) provide the simplest possible parametrization of the resonance part of the S matrix for a given number and type of resonances on the uniformization w plane keeping unitarity and analyticity. The free parameters (the zeros w_r) of the S_{res} with a particular number and type of resonances, are fixed by fitting to the experimental data. The scenario with the smallest χ^2 is chosen as the most probable hypothesis on the condition of the given data set. Note that this is an opposite approach to that, e.g., in Refs. [16,17] where the S matrix is constructed in the physical region and then it is analytically continued to the Riemann surface to find poles, for example, the σ -meson pole. In our approach, positions of the poles are obtained directly from the fitting. An optimal number of poles is the minimal number which guarantees a satisfactory description of the data and which contains only the poles significantly improving the fit. The poles are introduced according to the formulas for analytic continuations of the S -matrix elements to all sheets [2,11].

The background part S_{bgr} is constructed in the physical region to mimic an influence of the other singularities not included explicitly in the resonance part S_{res} . The simple form in Eq. (5) includes a response to the opening of the channels whose threshold branch points are not taken into account explicitly in the uniformizing variable. Values of the fitted parameters in Eq. (5) (a and b) indicate a relative importance of these branch points; e.g., a negative or large value of some background parameter could suggest that the corresponding branch point should be explicitly allowed for in the uniformizing variable. Therefore, in choosing the best variant we also require that the background contribution is negligible, i.e., the background parameters are small.

In our previous analysis of data on $\pi\pi \rightarrow \pi\pi, K\bar{K}$, we took into account the left-hand branch point at $s = 0$ in the uniformizing variable in addition to the $\pi\pi$ - and $K\bar{K}$ -threshold branch points [6]. In the analysis of $\pi\pi \rightarrow \pi\pi, K\bar{K}, \eta\eta$ we allowed rather for the $\eta\eta$ -threshold branch point [2]. In the presented more elaborate three-channel analysis, unlike in Ref. [2], we follow more consistently the spirit of the model-independent description obtaining practically zero background of the $\pi\pi$ scattering.

III. ANALYSIS OF THE DATA ON ISOSCALAR S-WAVE PROCESSES $\pi\pi \rightarrow \pi\pi, K\bar{K}, \eta\eta$ AND ON DECAYS $J/\psi \rightarrow \phi\pi\pi, \phi K\bar{K}$

In the combined analysis of data on the isoscalar S waves of processes $\pi\pi \rightarrow \pi\pi, K\bar{K}, \eta\eta$ [18–23] we added data on decays $J/\psi \rightarrow \phi\pi\pi, \phi K\bar{K}$ from the Mark III [7], DM2 [8], and BES II [9] Collaborations. Formalism for calculating the di-meson mass distributions of these decays can be found in Refs. [13,14]. In this approach, the pairs of the pseudoscalar mesons in the final states are assumed to have $I = J = 0$ and they undergo strong interactions whereas the ϕ meson behaves as a spectator. The amplitudes for $J/\psi \rightarrow \phi\pi\pi, \phi K\bar{K}$ decays are related with the scattering amplitudes T_{ij} $i, j = 1 - \pi\pi, 2 - K\bar{K}$ as follows:

$$F(J/\psi \rightarrow \phi\pi\pi) = \sqrt{2/3}[c_1(s)T_{11} + c_2(s)T_{21}], \quad (7)$$

$$F(J/\psi \rightarrow \phi K\bar{K}) = \sqrt{1/2}[c_1(s)T_{12} + c_2(s)T_{22}], \quad (8)$$

where $c_1 = \gamma_{10} + \gamma_{11}s$ and $c_2 = \kappa_2/(s - \lambda_2) + \gamma_{20} + \gamma_{21}s$ are functions of the couplings of the J/ψ to channels 1 and 2; $\kappa_2, \lambda_2, \gamma_{i0}$ and γ_{i1} are free parameters. The pole term in c_2 approximates possible ϕK states which are not forbidden by the Okubo-Zweig-Iizuka rule considering quark diagrams of these processes. Obviously this pole should be situated on the real s axis below the $\pi\pi$ threshold. This is an effective inclusion of the effect of so-called ‘‘crossed channel final-state interactions’’ in $J/\psi \rightarrow \phi K\bar{K}$, which was studied largely, e.g., in Ref. [24]. The di-meson mass distributions are given as

$$N|F|^2 \sqrt{(s - s_i)(m_\psi^2 - (\sqrt{s} - m_\phi)^2)(m_\psi^2 - (\sqrt{s} + m_\phi)^2)}, \quad (9)$$

where N is a normalization constant to data of the experiments determined in the analysis: 0.7512, 0.2783, and 5.699 for the Mark III, DM2, and BES II data, respectively. Parameters of the c_i functions, obtained in the analysis, are $\kappa_2 = 0.0843 \pm 0.0298$, $\lambda_2 = 0.0385 \pm 0.0251$, $\gamma_{10} = 1.1826 \pm 0.1430$, $\gamma_{11} = 1.2798 \pm 0.1633$, $\gamma_{20} = -1.9393 \pm 0.1703$, and $\gamma_{21} = -0.9808 \pm 0.1532$. The scattering amplitudes T_{ij} are related to the S matrix as

$$S_{ij} = \delta_{ij} + 2i\sqrt{\rho_i\rho_j}T_{ij}, \quad (10)$$

where $\rho_j = \sqrt{1 - 4m_j^2/s}$.

In the analysis we supposed that in the 1500-MeV region there are two resonances: the narrow $f_0(1500)$ and wide $f'_0(1500)$. The $f_0(500)$ state is described by the cluster of type (a), $f_0(1500)$ by type (c), and $f'_0(1500)$ by type (g). The $f_0(980)$ is represented only by the pole on sheet II and shifted pole on sheet III. However, the representation of the $f_0(1370)$ and $f_0(1710)$ states is not unique. These states

can be described by clusters either of type (b) or type (c). Analyzing only the processes $\pi\pi \rightarrow \pi\pi, K\bar{K}, \eta\eta(\eta\eta')$, similarly as it was done in [2], it is impossible to prefer any of four indicated possibilities. Moreover, it was found that the data admit two sets of parameters of $f_0(500)$ with a mass relatively near to the ρ -meson mass, and with the total widths either ≈ 600 or ≈ 930 MeV, solutions A and B, respectively, like in Ref. [2].

In the extended combined analysis, adding the data on decays $J/\psi \rightarrow \phi\pi\pi, \phi K\bar{K}$, one can prefer the scenarios when the $f_0(1370)$ is described by the cluster of type (b) and $f_0(1710)$ by the cluster of type either (b) or (c). To be specific, in the following we shall discuss the case when the $f_0(1710)$ is represented by the cluster of type (c).

It is interesting that the di-pion mass distribution of the $J/\psi \rightarrow \phi\pi\pi$ decay of the BES II data from the threshold to ≈ 0.85 GeV clearly prefers the solution with the wider $f_0(500)$ (solution B). A satisfactory description of all analyzed processes is obtained with the total $\chi^2/\text{NDF} = 407.402/(389 - 51) \approx 1.21$ where for the $\pi\pi$ scattering, $\chi^2/\text{NDF} \approx 1.15$, for $\pi\pi \rightarrow K\bar{K}$, $\chi^2/\text{NDF} \approx 1.65$, for $\pi\pi \rightarrow \eta\eta$, $\chi^2/\text{ndp} \approx 0.87$, and for decays $J/\psi \rightarrow \phi(\pi\pi, K\bar{K})$, $\chi^2/\text{ndp} \approx 1.21$.

The combined description (χ^2) of processes $\pi\pi \rightarrow \pi\pi, K\bar{K}, \eta\eta$ with adding the data on decays $J/\psi \rightarrow \phi(\pi\pi, K\bar{K})$ is practically the same as in Ref. [2], performed without considering decays of the J/ψ mesons. A comparison of the description with the experimental data is shown in Figs. 1–6.

In Table I we show the obtained pole clusters for the resonances on the complex-energy plane \sqrt{s} . The poles on sheets III, V, and VII and VI, corresponding to the $f'_0(1500)$, are of the second and third order, respectively (this is an approximation).

The pole positions of the $f_0(500)$, $f_0(1370)$, and $f_0(1710)$ have changed with respect to Ref. [2], especially the first one. The pole cluster of $f_0(980)$ practically did not change.

The obtained background parameters are $a_{11} = 0.0$, $a_{1\sigma} = 0.0199 \pm 0.0052$, $a_{1v} = 0.0$, $b_{11} = b_{1\sigma} = 0.0$, $b_{1v} = 0.0338 \pm 0.0099$, $a_{21} = -2.4649 \pm 0.0231$, $a_{2\sigma} = -2.3222 \pm 0.1587$, $a_{2v} = -6.611 \pm 0.5518$, $b_{21} = b_{2\sigma} = 0.0$, $b_{2v} = 7.073 \pm 1.287$, $b_{31} = 0.6421 \pm 0.0452$, $b_{3\sigma} = 0.4851 \pm 0.1011$, $b_{3v} = 0$; $s_\sigma = 1.6338$ GeV², $s_v = 2.08571$ GeV². The very simple description of the $\pi\pi$ -scattering background confirms well our assumption in Eq. (2). It is important that we have obtained practically zero background of the $\pi\pi$ scattering in the scalar-isoscalar channel because a reasonable and simple description of the background should be a criterion of correctness of the approach. Furthermore, this shows that the consideration of the left-hand branch point at $s = 0$ in the uniformizing variable solves partly the problem of some approaches (see, e.g., [26]) that the wide-resonance parameters are strongly controlled by the nonresonant background. Note also that

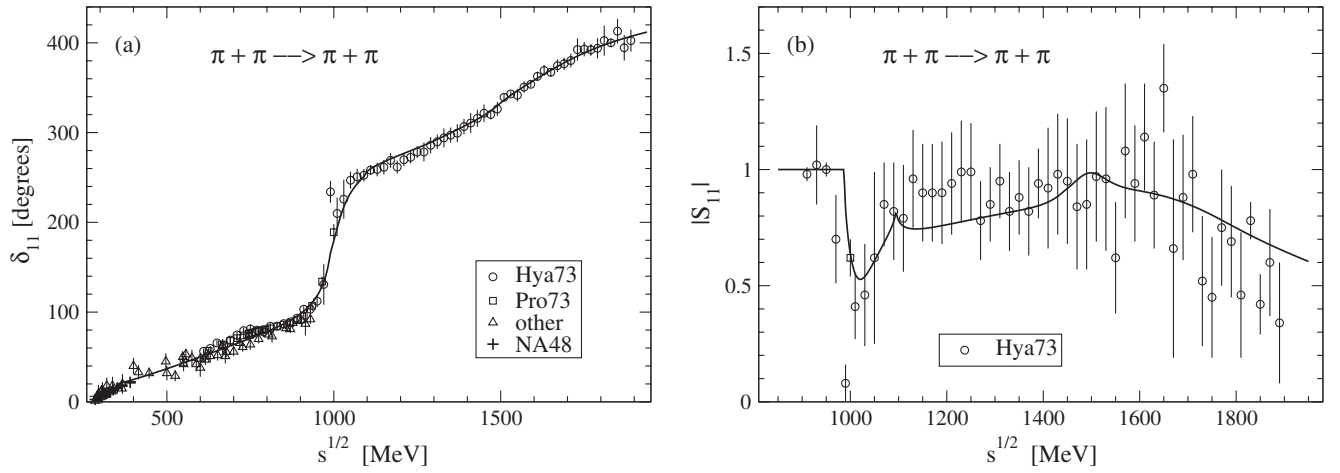


FIG. 1. The phase shift (a) and module (b) of the $\pi\pi$ -scattering S -wave matrix element. The data are from Ref. [18] (Hya73), [20] (Pro73), [19] (other), and [25] (NA48).

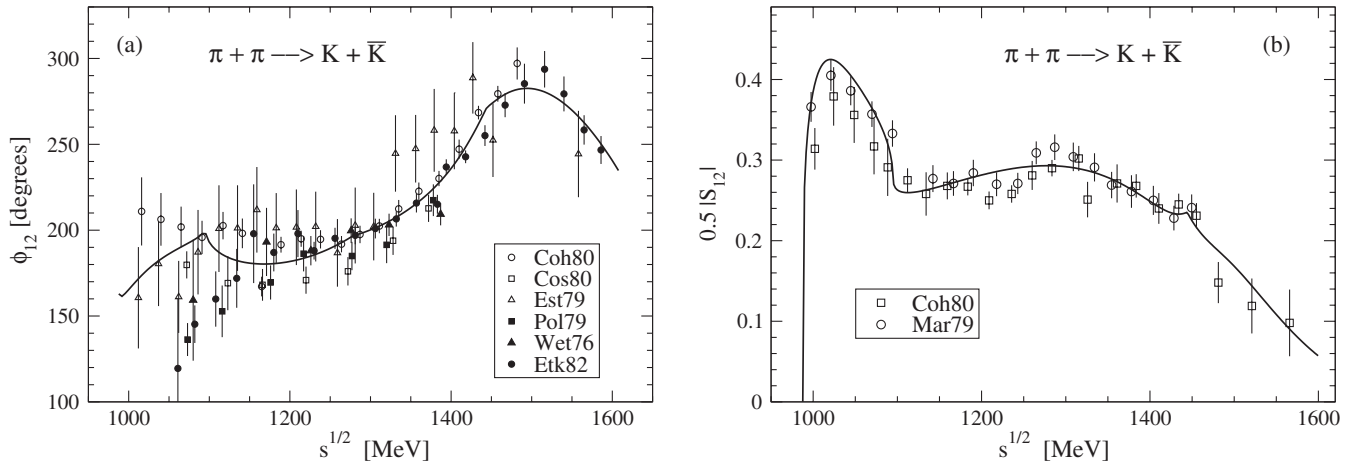


FIG. 2. The phase shift (a) and module (b) of the $\pi\pi \rightarrow K\bar{K}$ S -wave matrix element. The data are from Ref. [22] (Coh80, Cos80, Pol79, Wet76, Etk82, and Mar79) and [21] (Est79).

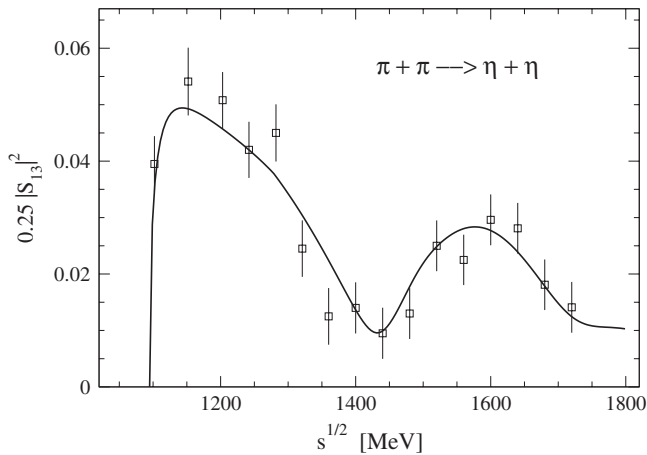


FIG. 3. The squared modules of the $\pi\pi \rightarrow \eta\eta$ S -wave matrix element. The data are from [23].

the zero background of the $\pi\pi$ scattering, in addition to the fact that $f_0(500)$ is described by the cluster, indicates this state to be the resonance (not a dynamically generated state). The point is that after the account of the left-hand branch point at $s = 0$, the remaining contributions of the crossed u and t channels are meson exchanges. The elastic background of the $\pi\pi$ scattering is related mainly to contributions of the crossed channels. Its zero value means that the exchange by the nearest ρ meson is obliterated by the exchange by a particle of near mass contributing with the opposite sign [the scalar $f_0(500)$] [27].

Generally, the wide multichannel states are most adequately represented by pole clusters located in a specific way on the Riemann surface because these clusters give the main model-independent contribution of the resonances [27]. Positions of the poles are rather stable characteristics for various models, whereas masses and widths are very

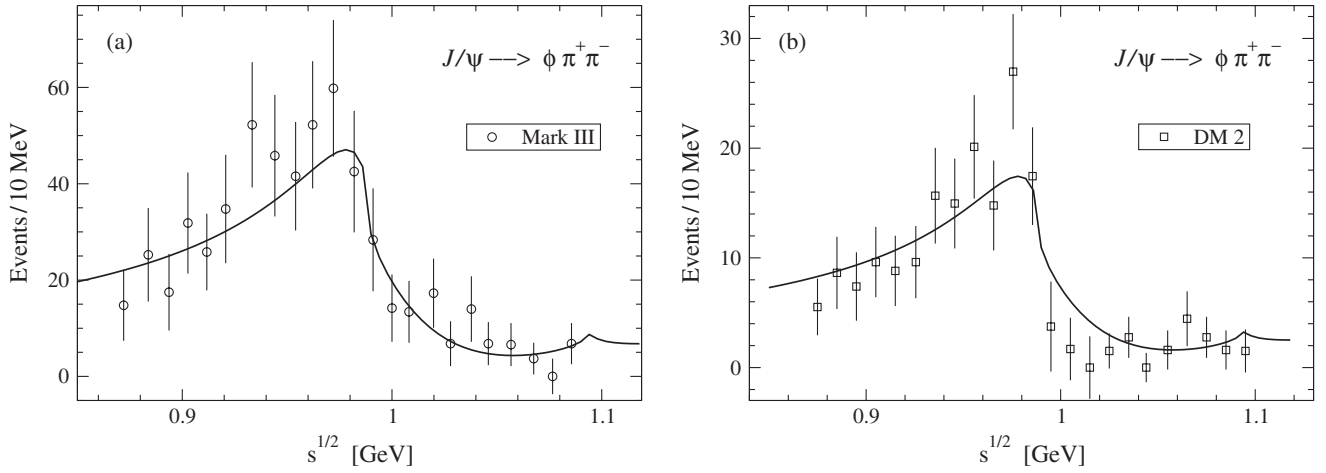


FIG. 4. The $\pi^+\pi^-$ invariant mass distributions in the $J/\psi \rightarrow \phi\pi^+\pi^-$ decay. Panel (a) shows the fit to the data of Mark III and (b) to DM2.

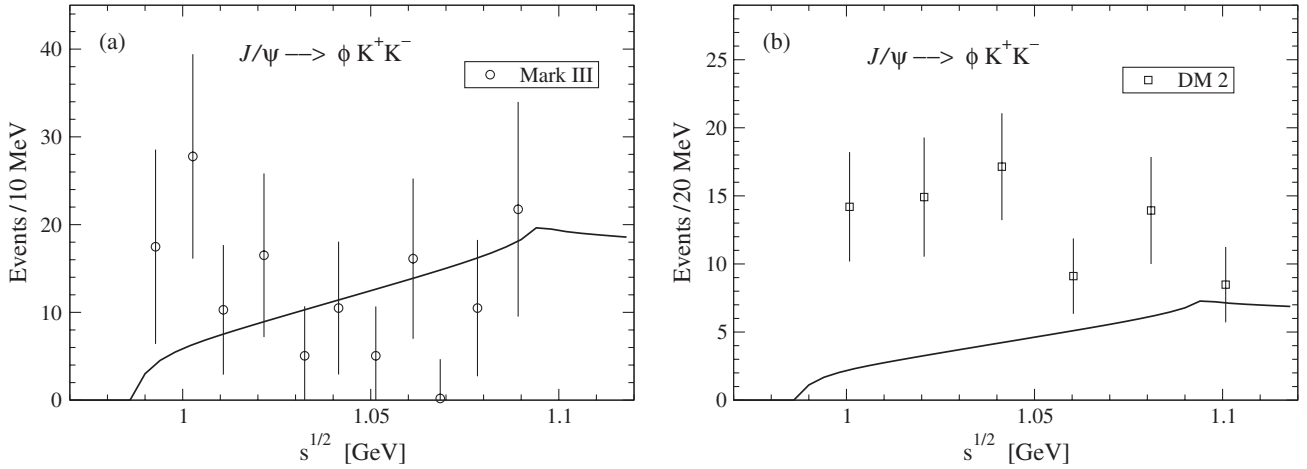


FIG. 5. The K^+K^- invariant mass distributions in the $J/\psi \rightarrow \phi K^+K^-$ decay. Panel (a) shows the fit to the data of Mark III and (b) to DM2.

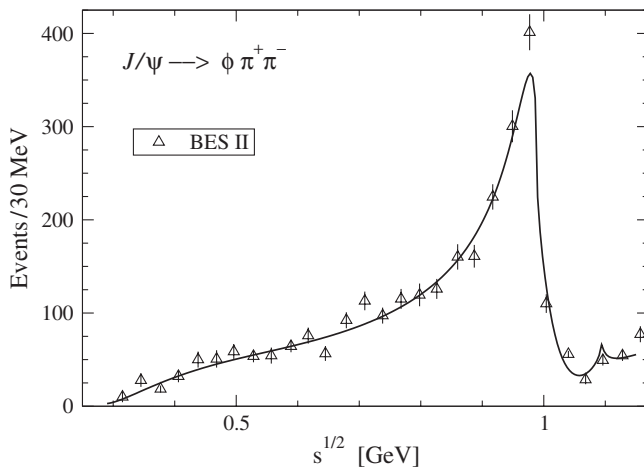


FIG. 6. The $\pi^+\pi^-$ invariant mass distribution in the $J/\psi \rightarrow \phi\pi^+\pi^-$ decay in comparison with the data of the BES II Collaboration.

model dependent for the wide resonances. However, values of masses are needed, e.g., in the mass relations for multiplets. In accordance with the discussion in Sec. II, we emphasize that the masses should be calculated using the poles on sheets II, IV, and VIII in dependence on the resonance classification. Here we use the formulas

$$T^{\text{res}} = \sqrt{s}\Gamma_{el}/(m_{\text{res}}^2 - s - i\sqrt{s}\Gamma_{\text{tot}}), \quad (11)$$

$$m_{\text{res}} = \sqrt{E_r^2 + (\Gamma_r/2)^2} \quad \text{and} \quad \Gamma_{\text{tot}} = \Gamma_r, \quad (12)$$

where E_r and $\Gamma_r/2$ are given in Table I. The calculated masses and widths for the f_0 states are shown in Table II. Let us note again that the mass of very broad resonances, $f_0(500)$, strongly depends on the used formula.

TABLE I. The pole clusters for resonances on the \sqrt{s} plane. $\sqrt{s_r} = E_r - i\Gamma_r/2$ in MeV.

Sheet		$f_0(500)$	$f_0(980)$	$f_0(1370)$	$f_0(1500)$	$f'_0(1500)$	$f_0(1710)$
II	E_r	514.5 ± 12.4	1008.1 ± 3.1			1512.7 ± 4.9	
	$\Gamma_r/2$	465.6 ± 5.9	32.0 ± 1.5			285.8 ± 12.9	
III	E_r	544.8 ± 17.7	976.2 ± 5.8	1387.6 ± 24.4		1506.2 ± 9.0	
	$\Gamma_r/2$	465.6 ± 5.9	53.0 ± 2.6	166.9 ± 41.8		127.9 ± 10.6	
IV	E_r			1387.6 ± 24.4		1512.7 ± 4.9	
	$\Gamma_r/2$			178.5 ± 37.2		216.0 ± 17.6	
V	E_r			1387.6 ± 24.4	1493.9 ± 3.1	1498.9 ± 7.2	1732.8 ± 43.2
	$\Gamma_r/2$			260.9 ± 73.7	72.8 ± 3.9	142.2 ± 6.0	114.8 ± 61.5
VI	E_r	566.5 ± 29.1		1387.6 ± 24.4	1493.9 ± 5.6	1511.4 ± 4.3	1732.8 ± 43.2
	$\Gamma_r/2$	465.6 ± 5.9		249.3 ± 83.1	58.4 ± 2.8	179.1 ± 4.0	111.2 ± 8.8
VII	E_r	536.2 ± 25.5			1493.9 ± 5.0	1500.5 ± 9.3	1732.8 ± 43.2
	$\Gamma_r/2$	465.6 ± 5.9			47.8 ± 9.3	99.7 ± 18.0	55.2 ± 38.0
VIII	E_r				1493.9 ± 3.2	1493.9 ± 3.2	1732.8 ± 43.2
	$\Gamma_r/2$				62.2 ± 9.2	299.6 ± 14.5	58.8 ± 16.4

TABLE II. Masses and total widths of the f_0 states.

	$f_0(500)$	$f_0(980)$	$f_0(1370)$	$f_0(1500)$	$f'_0(1500)$	$f_0(1710)$
m_{res} [MeV]	693.9 ± 10.0	1008.1 ± 3.1	1399.0 ± 24.7	1495.2 ± 3.2	1539.5 ± 5.4	1733.8 ± 43.2
Γ_{tot} [MeV]	931.2 ± 11.8	64.0 ± 3.0	357.0 ± 74.4	124.4 ± 18.4	571.6 ± 25.8	117.6 ± 32.8

IV. DISCUSSION OF THE RESULTS AND CONCLUSIONS

In the combined model-independent analysis of data on $\pi\pi \rightarrow \pi\pi, K\bar{K}, \eta\eta$ in the $I^G J^{PC} = 0^+ 0^{++}$ channel and on $J/\psi \rightarrow \phi\pi\pi, \phi K\bar{K}$ from the Mark III, DM2, and BES II Collaborations, an additional confirmation of the $f_0(500)$ with the pole at $514.5 \pm 12.4 - i(465.6 \pm 5.9)$ MeV on sheet II is obtained, which can be related with the mass 694 ± 10 MeV and width 931 ± 12 MeV via Eq. (12). The real part of the pole is in a good agreement with the results of other analyses cited in the PDG tables of 2012: The PDG estimation for the $f_0(500)$ pole is $(400\text{--}550) - i(200\text{--}350)$ MeV. The obtained imaginary part is, however, larger than the PDG estimation. As large values of the imaginary part of the $f_0(500)$ pole appear to be inherent in our method of analysis [2,28], the origin of this interesting result should be understood. In Ref. [28] we showed that a relatively narrow σ meson consistent with PDG can be obtained in the analysis of one-channel $\pi\pi$ scattering data but the inclusion of the $K\bar{K}$ data into the analysis makes the width significantly larger. Therefore it seems that the large width is tightly connected with the multichannel analysis of data. The value of the mass, which gets a significant contribution from the large width, Eq. (12), agrees well with the prediction by Weinberg in Ref. [29]. In this work it was shown that even where the chiral symmetry is spontaneously broken it can still be used to classify hadron states. Such mended symmetry leads to a quartet of particles with definite mass relations and C parity, giving

the prediction $m_\sigma \approx m_\rho$. This prediction is also in agreement with a refined analysis using the large- N_c consistency conditions between the unitarization and resonance saturation which suggests $m_\rho - m_\sigma = O(N_c^{-1})$ [30]. In addition, in the soft-wall anti-de Sitter/QCD approach [31]—the approach based on gauge/gravity duality—the predicted mass of the lowest f_0 meson, 721 MeV, practically coincides with the value obtained in our work. The above discussion concerns solution B, which is preferred by the analysis presented in this paper. The imaginary part of the $f_0(500)$ pole in solution A (343 MeV) [2] is still in agreement with the PDG estimation. However, solution A is inconsistent with data on the $J/\psi \rightarrow \phi\pi\pi$ decay from the BES II Collaboration: The corresponding curve in Fig. 6 lies considerably below the data from the threshold to about 850 MeV. Therefore, solution A is not considered in this paper. Anyway, the question of too large width of the $f_0(500)$ deserves a further investigation, estimating the theoretical uncertainties of our approach.

The obtained results for $f_0(980)$, $m_{\text{res}} = 1008 \pm 3$ MeV and $\Gamma_{\text{tot}} = 64 \pm 3$ MeV, indicate that the $f_0(980)$ is a non- $q\bar{q}$ state, e.g., the $\eta\eta$ bound state because it lies slightly above the $K\bar{K}$ threshold and is described by the pole on sheet II and by the shifted pole on sheet III without the corresponding (for standard clusters) poles on sheets VI and VII. In the PDG tables of 2010 its mass is 980 ± 10 MeV. We found in all combined analyses of the multichannel $\pi\pi$ scattering the $f_0(980)$ is slightly above 1 GeV, as in the dispersion-relations analysis only of the $\pi\pi$ scattering [32]. In the PDG tables of 2012, for the mass of

$f_0(980)$ an important alteration appeared: Now there is given the estimation 990 ± 20 MeV.

We conclude that the $f_0(1370)$ and $f_0(1710)$ states are dominated by the $s\bar{s}$ component in the wave function. The conclusion about the $f_0(1370)$ agrees with results of the work of the Crystal Barrel Collaboration [33] where the $f_0(1370)$ is identified as the $\eta\eta$ resonance in the $\pi^0\eta\eta$ final state of the $\bar{p}p$ annihilation at rest. This also explains well why one did not find this state considering only the $\pi\pi$ scattering process [4]. The conclusion about the $f_0(1710)$ is consistent with the experimental fact that this state is observed in $\gamma\gamma \rightarrow K_S K_S$ [34] but it is not observed in $\gamma\gamma \rightarrow \pi^+\pi^-$ [35].

In the 1500-MeV region, indeed, there are two states: the $f_0(1500)$ ($m_{\text{res}} \approx 1495$ MeV, $\Gamma_{\text{tot}} \approx 124$ MeV) and the $f'_0(1500)$ ($m_{\text{res}} \approx 1539$ MeV, $\Gamma_{\text{tot}} \approx 574$ MeV). The $f'_0(1500)$ is interpreted as a glueball taking into account its biggest width among the enclosing states [36]. As to the large width of the glueball, it is worth indicating Ref. [37]. There an effective QCD Lagrangian with the broken scale and chiral symmetry is used, where a glueball is introduced to theory as a dilaton and its existence is related to the breaking of scale symmetry in QCD. The $\pi\pi$ decay width of the glueball, estimated using low-energy theorems, is $\Gamma(G \rightarrow \pi\pi) \approx 0.6 \text{ GeV} \times (m_G/1 \text{ GeV})^5$ where m_G is the glueball mass. That is, if the glueball with the mass of about 1 GeV exists, then its width would be near 600 MeV. Of course, the use of the above formula is doubtful above 1 GeV; however, a trend for the glueball to be wide is apparently seen. On the other hand, in a two-flavor linear sigma model with global chiral symmetry and (axial-) vector mesons as well as an additional glueball degree of freedom where the glueball is also introduced as a dilaton [38], there arises the rather narrow resonance in the 1500-MeV region as predominantly a glueball with a subdominant qq component. On second thoughts, this result can be considered as preliminary due to using a quite rough flavor-symmetry $SU(N_f = 3)$ in the calculations or, e.g., evaluating the 4π decay, the intermediate state

consisting of two $f_0(500)$ mesons is not included. In Ref. [39], where the two-pseudoscalar and two-photon decays of the scalars between 1–2 GeV were analyzed in the framework of a chiral Lagrangian and the glueball was included as a flavor-blind composite mesonic field, the glueball was found to be rather narrow.

Taking into account the discovery of isodoublet $K_0^*(800)$ [1] (see also [40]), two lower nonets should correspond to two existing isodoublets K_0^* . We propose the following sets of the $SU(3)$ partners for these states excluding the $f_0(980)$ as the non- $q\bar{q}$ state [2]: The lowest nonet consists of the isovector $a_0(980)$, the isodoublet $K_0^*(800)$, and $f_0(500)$ and $f_0(1370)$ as mixtures of the eighth component of the octet and the $SU(3)$ singlet. The next nonet could consist of the isovector $a_0(1450)$, the isodoublet $K_0^*(1450)$, and two isoscalars $f_0(1500)$ and $f_0(1710)$. Since this assignment removes a number of questions that stood earlier when placing the scalar mesons to nonets and does not put forth any new ones, we think this is the right direction. An adequate mixing scheme is needed, the search for which is complicated by the fact that, in this case, there is also a remainder of chiral symmetry which, however, makes it possible to predict correctly, e.g., the σ -meson mass [29].

ACKNOWLEDGMENTS

The authors thank Thomas Gutsche and Mikhail Ivanov for useful discussions and interest in this work. This work was supported in part by the Grant Program of Plenipotentiary of the Slovak Republic at JINR, the Heisenberg-Landau Program, the Votruba-Blokhintsev Program for Cooperation of the Czech Republic with JINR, the Grant Agency of the Czech Republic (Grant No. P203/12/2126), the Bogoliubov-Infeld Program for Cooperation of Poland with JINR, the DFG under Contract No. LY 114/2-1. The work was also partially supported under the project 2.3684.2011 of Tomsk State University. This work has been partly supported by the Polish NCN Grant No. 2013/09/B/ST2/04382.

-
- [1] J. Beringer *et al.* (Particle Data Group), *Phys. Rev. D* **86**, 010001 (2012).
 [2] Yu. S. Surovtsev, P. Bydžovský, and V. E. Lyubovitskij, *Phys. Rev. D* **85**, 036002 (2012).
 [3] D. Bugg, *Eur. Phys. J. C* **52**, 55 (2007).
 [4] W. Ochs, *AIP Conf. Proc.* **1257**, 252 (2010); P. Minkowski and W. Ochs, *Eur. Phys. J. C* **9**, 283 (1999); *Nucl. Phys. B, Proc. Suppl.* **121**, 119 (2003); **121**, 123 (2003).
 [5] L. S. Geng and E. Oset, *Phys. Rev. D* **79**, 074009 (2009).
 [6] Yu. S. Surovtsev, P. Bydžovský, R. Kamiński, V. E. Lyubovitskij, and M. Nagy, *J. Phys. G* **41**, 025006 (2014).
 [7] W. Lockman, *Proceedings of the Hadron '89 Conference*, edited by F. Binon *et al.* (Editions Frontières, Gif-sur-Yvette, 1989) p. 109.
 [8] A. Falvard *et al.*, *Phys. Rev. D* **38**, 2706 (1988).
 [9] M. Ablikim *et al.*, *Phys. Lett. B* **607**, 243 (2005).
 [10] V. V. Anisovich, *Int. J. Mod. Phys. A* **21**, 3615 (2006).
 [11] D. Krupa, V. A. Meshcheryakov, and Yu. S. Surovtsev, *Nuovo Cimento A* **109**, 281 (1996).
 [12] Yu. S. Surovtsev, P. Bydžovský, T. Gutsche, R. Kamiński, V. E. Lyubovitskij, and M. Nagy, [arXiv:1311.1066](https://arxiv.org/abs/1311.1066).
 [13] D. Morgan and M. R. Pennington, *Phys. Rev. D* **48**, 1185 (1993); **48**, 5422 (1993).

- [14] B.S. Zou and D.V. Bugg, *Phys. Rev. D* **50**, 591 (1994).
- [15] K.J. Le Couteur, *Proc. R. Soc. A* **256**, 115 (1960); R.G. Newton, *J. Math. Phys. (N.Y.)* **2**, 188 (1961); M. Kato, *Ann. Phys. (N.Y.)* **31**, 130 (1965).
- [16] I. Caprini, *Phys. Rev. D* **77**, 114019 (2008).
- [17] I. Caprini, G. Colangelo, and H. Leutwyler, *Phys. Rev. Lett.* **96**, 132001 (2006).
- [18] B. Hyams *et al.*, *Nucl. Phys.* **B64**, 134 (1973); **B100**, 205 (1975).
- [19] A. Zylbersztejn, P. Basile, M. Bourquin, J.P. Boymond, A. Diamant-Berger, P. Extermann, P. Kunz, R. Mermod, H. Suter, and R. Turlay, *Phys. Lett.* **38B**, 457 (1972); P. Sonderegger and P. Bonamy, in *Proceedings of the 5th International Conference on Elementary Particles, Lund, 1969*, edited by G. von Dardel (Berlingska Boktryckeriet, Lund, Sweden, 1970) p. 372; J.R. Bensinger, A.R. Erwin, M.A. Thompson, and W.D. Walker, *Phys. Lett.* **36B**, 134 (1971); J.P. Baton, G. Laurens, and J. Reignier, *Phys. Lett.* **33B**, 525 (1970); **33B**, 528 (1970); P. Baillon, R.K. Carnegie, E.E. Kluge, D.W.G.S. Leith, H.L. Lynch, B. Ratcliff, B. Richter, H.H. Williams, and S.H. Williams, *Phys. Lett.* **38B**, 555 (1972); L. Rosselet *et al.*, *Phys. Rev. D* **15**, 574 (1977); A.A. Kartamyshev *et al.*, *Pis'ma Zh. Eksp. Theor. Fiz.* **25**, 68 (1977); A.A. Bel'kov *et al.*, *Pis'ma Zh. Eksp. Theor. Fiz.* **29**, 652 (1979).
- [20] S.D. Protopopescu, M. Alston-Garnjost, A. Barbaro-Galtieri, S. Flatté, J. Friedman, T. Lasinski, G. Lynch, M. Rabin, and F. Solmitz, *Phys. Rev. D* **7**, 1279 (1973).
- [21] P. Estabrooks and A.D. Martin, *Nucl. Phys.* **B79**, 301 (1974).
- [22] W. Wetzel, K. Freudenreich, F.X. Gentit, P. Muhlemann, W. Beusch, A. Birman, D. Websdale, P. Astbury, A. Harckham, and M. Letheren, *Nucl. Phys.* **B115**, 208 (1976); V.A. Polychronakos, N. Cason, J. Bishop, N. Biswas, V. Kenney, D. Rhines, R. Ruchti, W. Shephard, M. Stangl, and J. Watson, *Phys. Rev. D* **19**, 1317 (1979); P. Estabrooks, *Phys. Rev. D* **19**, 2678 (1979); D. Cohen, D. Ayres, R. Diebold, S. Kramer, A. Pawlicki, and A. Wicklund, *Phys. Rev. D* **22**, 2595 (1980); G. Costa *et al.*, *Nucl. Phys.* **B175**, 402 (1980); A. Etkin *et al.*, *Phys. Rev. D* **25**, 1786 (1982); A.D. Martin and E.N. Ozmutlu, *Nucl. Phys.* **B158**, 520 (1979).
- [23] F. Binon *et al.*, *Nuovo Cimento A* **78**, 313 (1983).
- [24] B. Liu, M. Buescher, F.-K. Guo, C. Hanhart, and U.-G. Meissner, *Eur. Phys. J. C* **63**, 93 (2009).
- [25] J.R. Batley *et al.*, *Eur. Phys. J. C* **54**, 411 (2008).
- [26] N.N. Achasov and G.N. Shestakov, *Phys. Rev. D* **49**, 5779 (1994).
- [27] Yu. S. Surovtsev, D. Krupa, and M. Nagy, *Eur. Phys. J. A* **15**, 409 (2002); *Czech. J. Phys.* **56**, 807 (2006).
- [28] Yu. S. Surovtsev, P. Bydžovský, R. Kamiński, V.E. Lyubovitskij, and M. Nagy, *Phys. Rev. D* **86**, 116002 (2012).
- [29] S. Weinberg, *Phys. Rev. Lett.* **65**, 1177 (1990).
- [30] J. Nieves and E. Ruiz Arriola, *Phys. Rev. D* **80**, 045023 (2009).
- [31] T. Gutsche, V.E. Lyubovitskij, I. Schmidt, and A. Vega, *Phys. Rev. D* **87**, 056001 (2013).
- [32] R. García-Martín, R. Kamiński, J.R. Peláez, and J.R. de Elvira, *Phys. Rev. Lett.* **107**, 072001 (2011).
- [33] C. Amsler *et al.*, *Phys. Lett. B* **355**, 425 (1995).
- [34] S. Braccini, in *Proceedings of the Workshop on Hadron Spectroscopy, Frascati, 1999*, edited by T. Bressani, A. Feliciello, and A. Filippi, *Frascati Phys. Series XV*, 53 (1999).
- [35] R. Barate *et al.*, *Phys. Lett. B* **472**, 189 (2000).
- [36] V.V. Anisovich *et al.*, *Nucl. Phys. Proc. Suppl. A* **56**, 270 (1997).
- [37] J. Ellis and J. Lánik, *Phys. Lett.* **150B**, 289 (1985).
- [38] S. Janowski, D. Parganlija, F. Giacosa, and D.H. Rischke, *Phys. Rev. D* **84**, 054007 (2011).
- [39] F. Giacosa, T. Gutsche, V.E. Lyubovitskij, and A. Faessler, *Phys. Rev. D* **72**, 094006 (2005).
- [40] Yu. S. Surovtsev, T. Branz, T. Gutsche, and V.E. Lyubovitskij, *Phys. Part. Nucl.* **41**, 990 (2010).